Optical coupling from InGaAs subcell to InGaP subcell in InGaP/InGaAs/Ge multi-junction solar cells

G. W. Shu,[1] J. Y. Lin,[2] H. T. Jian,[1] J. L. Shen,[1,5] S. C. Wang,[1] C. L. Chou,[1] W. C. Chou,[2] C. H. Wu,[3,5] C. H. Chiu,[4] and H. C. Kuo[4]

[1]*Department of Physics, Chung Yuan Christian University, Chung-Li 32023, Taiwan*
[2]*Department of Electrophysics, National Chiao Tung University, Hsin-chu 30010, Taiwan*
[3]*Institute of Nuclear Research, P. O. Box 3-11, Lungtan 32500, Taiwan*
[4]*Department of Photonic and Institute of Electro-Optical Engineering, National Chiao Tung University, Hsin-chu30010, Taiwan*
[5]*jlshen@cycu.edu.tw*
[*]*chung@iner.gov.tw*

Abstract: Spatially-resolved electroluminescence (EL) images in the triple-junction InGaP/InGaAs/Ge solar cell have been investigated to demonstrate the subcell coupling effect. Upon irradiating the infrared light with an energy below bandgap of the active layer in the top subcell, but above that in the middle subcell, the EL of the top subcell quenches. By analysis of EL intensity as a function of irradiation level, it is found that the coupled p-n junction structure and the photovoltaic effect are responsible for the observed EL quenching. With optical coupling and photoswitching effects in the multi-junction diode, a concept of infrared image sensors is proposed.

©2012 Optical Society of America

OCIS codes: (040.5350) Photovoltaic ; (260.3800) Luminescence.

References and links

1. S. Kurtz and J. Geisz, "Multijunction solar cells for conversion of concentrated sunlight to electricity," Opt. Express **18**(S1), A73–A78 (2010).
2. T. Fuyuki, H. Kondo, T. Yamazaki, Y. Takahashi, and Y. Uraoka, "Photographic surveying of minority carrier diffusion length in polycrystalline silicon solar cells by electroluminescence," Appl. Phys. Lett. **86**(26), 262108 (2005).
3. J. Giesecke, M. Kasemann, and W. Warta, "Determination of local minority carrier diffusion lengths in crystalline silicon from luminescence images," J. Appl. Phys. **106**(1), 014907 (2009).
4. P. Würfel, T. Trupke, T. Puzzer, E. Schäffer, W. Warta, and S. W. Glunz, "Diffusion lengths of silicon solar cells from luminescence images," J. Appl. Phys. **101**(12), 123110 (2007).
5. M. Glatthaar, J. Giesecke, M. Kasemann, J. Haunschild, M. The, W. Warta, and S. Rein, "Spatially resolved determination of the dark saturation current of silicon solar cells from electroluminescence images," J. Appl. Phys. **105**(11), 113110 (2009).
6. T. Fuyuki, H. Kondo, Y. Kaji, A. Ogane, and Y. Takahashi, "Analytic findings in the electroluminescence characterization of crystalline silicon solar cells," J. Appl. Phys. **101**(2), 023711 (2007).
7. T. Kirchartz, U. Rau, M. Hermle, A. W. Bett, A. Helbig, and J. H. Werner, "Internal voltage in GaInP/GaInAs/Ge multijunction solar cells determined by electroluminescence measurements," Appl. Phys. Lett. **92**(12), 123502 (2008).
8. S. Roensch, R. Hoheisel, F. Dimroth, and A. W. Bett, "Subcell I-V characteristic analysis of GaInP/GaInAa/Ge solar cells using electroluminescence measure;ments," Appl. Phys. Lett. **98**(25), 251113 (2011).
9. C. G. Zimmermann, "Utilizing lateral current spreading in multijunction solar cells: An alternative approach to detecting mechanical defects," J. Appl. Phys. **100**(2), 023714 (2006).
10. H. Takeuchi, Y. Kamo, Y. Yamamoto, T. Oku, M. Totsuka, and M. Nakayama, "Phoitovoltaic effects on Franz-Keldysh oscillation in photoreflectance spectra: Application to determination of surface Fermi level and surface recombination velocity in undoped GaAs/n-type GaAs epitaxial layer structures," J. Appl. Phys. **97**(6), 063708 (2005).
11. S. M. Sze, *Semiconductor Devices, Physics and Technology* (John Wiley & Sons Inc., 2002).
12. F. H. Pollak, "Study of semiconductor surfaces and interfaces using electromodulation," Surf. Interface Anal. **31**(10), 938–953 (2001).

#174226 - $15.00 USD Received 13 Aug 2012; revised 18 Nov 2012; accepted 25 Nov 2012; published 10 Dec 2012
(C) 2012 OSA

13. R. G. Rodriges, I. Bhat, J. M. Borrego, and R. Venkatasubramanian, "Photoreflectance characterization of InP and GaAs solar cells," in *Proceedings of IEEE Conference on Photovoltaic Specialists Conference* (IEEE, 1993), pp. 504–509.
14. M. Meusel, C. Baur, G. Létay, A. W. Bett, W. Warta, and E. Fernandez, "Spectral response measurements of monolithic GaInP/Ga(In)As/Ge triple-junction solar cells: measurement artifacts and their explanation," Prog. Photovolt. Res. Appl. **11**, 499 (2003).
15. S. H. Lim, J. J. Li, E. H. Steenbergen, and Y. H. Zhang, "Luminescence coupling effects on multijunction solar cell external quantum efficiency measurement," Prog. Photovolt. Res. Appl. (to be published).

1. Introduction

III-V compound multi-junction solar cells are complicated photovoltaic devices, which are promising for space and terrestrial applications and provide today's highest conversion efficiencies. Record efficiencies of more than 41% have been demonstrated under concentrated illumination [1]. While the subcells in multi-junction solar cells usually have separate contacts, they are monolithically integrated on one substrate and interconnected in series by tunnel diodes. Thus, operation of the subcells in multi-junction solar cells is not separated and independent, but couples with other subcells both electrically and optically. The interactions between the subcells are fundamental characteristics that can affect the conversion efficiency in multi-junction solar cells. For example, for a photon emitted from the active layer of a higher bandgap junction in high-quality multi-junction solar cells, there is a probability of it being reabsorbed in a lower bandgap junction, yielding a radiative coupling effect. This can produce unintentional photocurrent (luminescence coupling photocurrent) and cause measurement artifacts. Since most of III-V materials are direct semiconductors, where radiative recombination is the dominating recombination process, radiative coupling has a considerable impact on the performance or the behavior of a III-V multi-junction solar cell.

Among many characterization techniques, electroluminescence (EL) imaging has evolved to be an effective, nondestructive, and fast tool for spatially revolved characterization of electronic properties in solar cells [2-6]. For III-V multi-junction solar cells, the use of EL as a powerful characteristic tool has been reported. Due to the reciprocity theorem between EL emission and external quantum efficiency of solar cells, the individual current-voltage curves and the diode quality factors of all subcells were obtained in the triple-junction InGaP/InGaAs/Ge solar cells [7,8]. EL can also aid in the determination of surface recombination velocities, sheet resistances or carrier lifetime since EL correlates with the concentrations of the recombination centers existing in the subcell [9]. In this report, we propose that a coupling effect from a lower bandgap junction to a higher bandgap junction can be possible in InGaP/InGaAs/Ge solar cells. The electroluminescence (EL) imaging was used as a vehicle to verify the coupling from the InGaAs middle subcell to the InGaP top subcell. We demonstrate that the visible EL in the top subcell of the InGaP/InGaAs/Ge solar cells is quenched under illumination of the 1.59-eV infrared (IR) light, with an energy below the bandgap of InGaP, but above that of InGaAs. The quenching mechanism of EL was studied with different irradiation power of the IR light and analyzed by considering the photovoltaic effects. The optical coupling in the multi-junction diode may provide an idea for implementing the infrared image sensing.

2. Experiment

The samples investigated here were composed of cascade-type InGaP/InGaAs/Ge junctions connected in series. The top $In_{0.5}Ga_{0.5}P$, middle $In_{0.01}Ga_{0.99}As$, and bottom Ge subcells were all lattice-matched and grown on a p-type Ge substrate by metal-organic chemical vapor deposition (MOCVD). The InGaP subcell was connected to the InGaAs subcell by a p-AlGaAs/n-InGaP tunnel junction. The InGaAs subcell was connected to the Ge subcell by a p-GaAs/n-GaAs tunnel junction. Figure 1 shows the schematic and detailed doping concentrations of the triple-junction InGaP/InGaAs/Ge solar cell investigated in this study. EL images of the solar cell were performed under an appropriate forward bias at room

#174226 - $15.00 USD   Received 13 Aug 2012; revised 18 Nov 2012; accepted 25 Nov 2012; published 10 Dec 2012
(C) 2012 OSA

temperature. To produce the EL image, a Keithley 6430 source-meter was used as the current source. The images of top region of the solar cell were taken by a standard Si charge-coupled device (CCD) camera. The 1024 × 1024 pixel camera yields a resolution of ~6.5μm on the 5.5 × 5.5 mm^2 cell. The data acquisition time was chosen to be 1 ms. An IR filter to pass shorter than the wavelength of 775 nm was used to block the EL from the middle InGaAs subcell. An extra IR laser with wavelength (energy) of 780 nm (1.59 eV) was used to excite the electron-hole pairs in the active layer of the middle InGaAs subcell, affecting EL from the top subcell. A manually adjustable density filter was used to control the intensity of IR laser reaching the cell sample.

Type	Layer	Doping	
n	AlInP	$3 \times 10^{18}\ cm^{-3}$	Top cell
n	$In_{0.51}Ga_{0.49}P$	$2 \times 10^{18}\ cm^{-3}$	
p	$In_{0.51}Ga_{0.49}P$	$3 \times 10^{17}\ cm^{-3}$	
p	AlInP	$6 \times 10^{17}\ cm^{-3}$	
p^+	AlGaAs	$1 \times 10^{19}\ cm^{-3}$	Tunnel diode 1
n^+	InGaP	$1 \times 10^{19}\ cm^{-3}$	
n	AlInP	$3 \times 10^{18}\ cm^{-3}$	middle cell
n	$In_{0.01}Ga_{0.99}As$	$2 \times 10^{18}\ cm^{-3}$	
p	$In_{0.01}Ga_{0.99}As$	$3 \times 10^{17}\ cm^{-3}$	
p	InGaP	$3 \times 10^{18}\ cm^{-3}$	
p^+	GaAs	$1 \times 10^{19}\ cm^{-3}$	Tunnel diode 2
n^+	GaAs	$1 \times 10^{19}\ cm^{-3}$	
n	$In_{0.01}Ga_{0.99}As$	$2 \times 10^{17}\ cm^{-3}$	bottom cell
n	Ge	$3 \times 10^{18}\ cm^{-3}$	
p	Ge	$9 \times 10^{17}\ cm^{-3}$	

Fig. 1. Schematic illustration of the investigated InGaP/InGaAs/Ge triple-junction solar cell.

3. Results and discussion

The visible band-edge emission from the top InGaP subcell can be observed by EL. For producing EL images, a current density of 35 mA/cm^2 is driven by a current source through cell. Figure 2(a) shows the EL image of the InGaP subcell measured with a 775 nm short pass filter mounted in front of the CCD camera, revealing a homogenous image. The emitted red light was clearly seen by a naked eye in normal office light environment. Figure 2(b) displays the EL image by irradiating the IR light with energy below bandgap of the active-layer in the top subcell (InGaP), but above that in the middle subcell (InGaAs). A clear reduction of the EL intensity was observed around the spot of the incident light.

EL images generally provide spatial information on the material quality of solar cells, where dark areas exist owing to carrier recombination induced by defects [9]. However, quenching of EL by IR light irradiation is a reversible behavior (will be demonstrated later), excluding the possibility that the dark spot is owing to the poor material quality in solar cells. In the aim of a better comprehension on EL quenching, measurements of the light-current characteristics with (without) IR light irradiation were carried out. Figure 3 displays the light-current curve with (the dashed line) and without (the solid line) IR light irradiation. EL intensity from the top subcell is roughly linear after the current density > ~30 mA/cm^2. With IR light irradiation, we note that EL intensity decreases by about 40% at the current density of 35 mA/cm^2 (from point **o** to point **p**). On the other hand, the reduced EL intensity with IR irradiation (point **p**) can be considered as the EL intensity driven at lower current density (point **q**). Therefore, the effect of IR irradiation is equivalent to decrease the forward current density (from point **o** to point **q**), which leads to a decrease of EL intensity. This result indicates that although the EL is emitted from the top subcell, the coupling from the middle subcell have to be taken into account.

#174226 - $15.00 USD Received 13 Aug 2012; revised 18 Nov 2012; accepted 25 Nov 2012; published 10 Dec 2012
(C) 2012 OSA

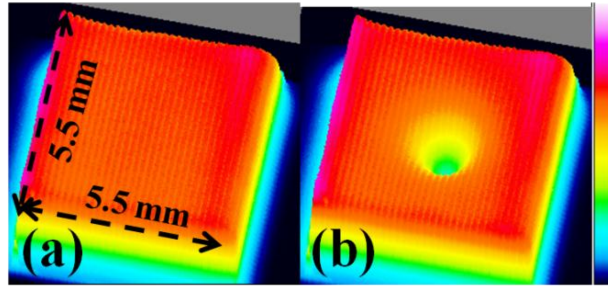

Fig. 2. Electroluminescence (EL) images of the triple-junction InGaP/InGaAs/Ge solar cell taken with the measurement (a) without and (b) with irradiation of an extra IR laser. The scale bar applies to images (a)-(b).

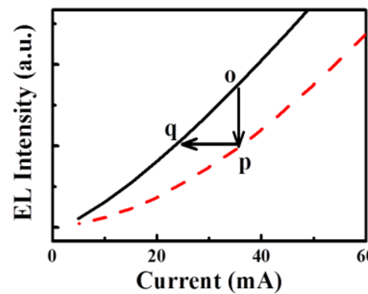

Fig. 3. The dependence of EL intensity of the top subcell on injection current without (the solid line) and with (the dashed line) irradiation of an extra IR laser.

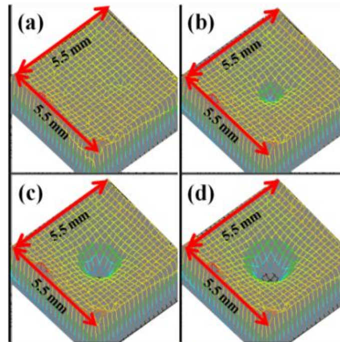

Fig. 4. Surface maps of EL intensity of the top subcell with different irradiation powers of IR light: (a) 0 (b) 1.8 (c) 8.3, and (d) 18.7 mW.

In order to investigate the mechanism of EL quenching, EL images as a function of the IR-light irradiation power were studied. Figure 4(a)-4(d) shows the variation of the EL intensity with illumination of IR laser under different irradiation powers. Circular features with reduced EL intensity around the laser spot were observed. The laser output power was varied from 0 to 87 mW. As the irradiation power increases, EL intensity decreases accordingly. Figure 5 displays the EL intensity profiles recorded along one dimension. The profile of the laser spot is also displayed in Fig. 5. EL intensity shows a considerable decrease with increasing the irradiation power, revealing an increase of the dark region in the EL image. We can quantitatively estimate the EL intensity by integrating the luminescence intensity detected in the CCD camera. Open circles in Fig. 6 plots the measured EL intensity as a function of the irradiation power. The integrated EL intensity decays exponentially with increasing the irradiation power of the IR light.

#174226 - $15.00 USD Received 13 Aug 2012; revised 18 Nov 2012; accepted 25 Nov 2012; published 10 Dec 2012
(C) 2012 OSA

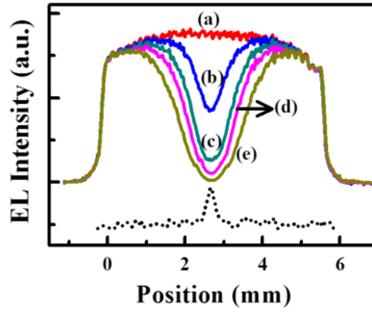

Fig. 5. EL intensity of profile of a line scan in the top subcell with different irradiation power of IR light: (a) 0, (b) 1.8, (c) 8.3, (d) 18.7, and (e) 59.0 mW. The dotted line displays the beam profile of the IR laser.

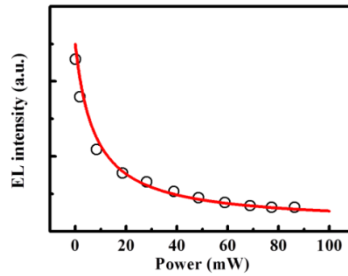

Fig. 6. Integrated EL intensity from a line scan versus the irradiation power of IR light.

The dependence of EL intensity on the irradiation power can be analyzed according to the p-n junction diode model. Under forward bias condition, EL intensity I_{EL} from the InGaP subcell is related to the solar-cell parameters by [6]:

$$I_{EL} \propto n_{p(0)} L, \tag{1}$$

where $n_{p(0)}$ is the excess minority carrier number at the p-n junction edge and L is the effective diffusion length. With an applied forward voltage V_{app}, $n_{p(0)}$ is given by the following equation [6]:

$$n_{p(0)} = n_p \exp(eV_{app} / kT), \tag{2}$$

where n_p is the equilibrium minority carrier density in the p base layer and k is Boltzmann constant. Combining Eqs. (1) and (2), EL intensity I_{EL} from a p-n junction can be expressed by V_{app} given as

$$\ln I_{EL} = C + eV_{app} / kT, \tag{3}$$

where C is a constant. This formula suggests that EL intensity can be tuned by the applied forward voltage.

In the next step, we describe how the IR irradiation affects the forward voltage in the top InGaP subcell. When the InGaP/InGaAs/Ge solar cell is illuminated by the IR light, a photovoltage owing to absorption of IR light is generated in the InGaAs subcell. According to the diode equation, the photovoltage V_{ph} can be represented by [10]

$$V_{ph} = \frac{nkT}{q} \ln(\frac{J_{PC}}{AJ_0} + 1), \tag{4}$$

#174226 - $15.00 USD Received 13 Aug 2012; revised 18 Nov 2012; accepted 25 Nov 2012; published 10 Dec 2012
(C) 2012 OSA

where n is an ideal factor, J_0 is the saturation current density, J_{PC} is the photocurrent density and A is a geometric factor. The photocurrent densities in Eq. (4) are associated with the drift and diffusion currents and can be simplified if the diffusion length greatly exceeds the penetration depth of light. In this case, the photocurrent density is expected to be proportional to the illumination power [11]:

$$J_{PC} = eP\eta(1-R)/\hbar\omega, \tag{5}$$

where P is the illumination power, η is the quantum efficiency, R is the reflectivity, and $\hbar\omega$ is the photon energy. To investigate the voltage change generated by the IR illumination, we have measured the electroreflectance spectra of the InGaP top subcell under different illumination power of IR light. For sufficiently high electric fields electroreflectance exhibits oscillatory patterns above the bandgap, the so-called Franz–Keldysh oscillations (FKOs). By fitting FKOs, the electric-field strength can be determined accurately [12]. The measured electroreflectance spectra of the InGaP top subcell without and with IR illumination are shown in Fig. 7. The spectra have FKOs that persist to several hundred meV above the bandgap critical point. It is found the distance between consecutive peaks of FKO increases for the spectrum with the IR illumination, indicating an increase of the electric field at the p-n junction. Based on FKO analysis [12], electric fields of 56 and 82 KV/cm are obtained without and with the IR illumination, respectively. In a fully depleted space charge region the square magnitude of the electric field in the junction is linear to the applied bias [13]. Thus, we can derive the induced voltage change δV from the electroreflectance measurements. The circles in Fig. 8 show δV of the InGaP top subcell for five different illumination powers. Obviously, the induced voltage increases monotonically with increasing the illumination power of IR light. On the other hand, by taking n = 2, $J_0 \sim 4.2\times10^{-14}$ A/cm^2 (Ref [14].), kT = 26 meV, and $A = 7\times10^{13}$, the photovoltage V_{ph} can be fitted according to Eq. (4). The solid line in Fig. 8 displays the fitted result, in good agreement with the induced voltage change δV. This indicates the IR illumination produces a photovoltage which acts as an applied bias to the InGaP top subcell.

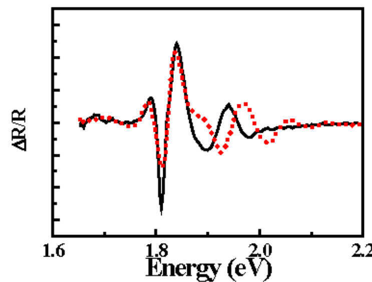

Fig. 7. Electroreflectance spectra of the InGaP top subcell without (the solid line) and with (the dotted line) the IR illumination of 20 mW.

#174226 - $15.00 USD   Received 13 Aug 2012; revised 18 Nov 2012; accepted 25 Nov 2012; published 10 Dec 2012
(C) 2012 OSA

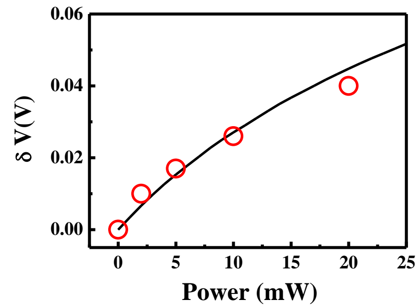

Fig. 8. Induced voltage change δV of the InGaP top subcell for five different illumination powers (open circles). The solid line displays the calculated photovoltage according to Eq. (4).

Now, we try to analyze EL quenching as a function of IR illumination power. Upon illumination of the IR light, V_{app} in Eq. (3) is replaced by V_{app}- V_{ph} owing to the photovoltaic effect:

$$\ln I_{EL} = C + e(V_{app} - V_{ph}) / kT . \tag{6}$$

According to Eqs. (4)-(6), EL of the top subcell can be estimated by considering the photovoltaic effect in the middle subcell. By taking V_{app} = 1.4V, the solid line in Fig. 6 displays the fitted EL intensity as a function of illumination power, revealing a good agreement with the experimental result. We hence conclude that EL quenching is induced from the decreased forward voltage (current) in the InGaP top subcell, originating from the photovoltaic effect in the InGaAs middle subcell. This result indicates that the p-n junction of the top subcell and that of the middle subcell are coupled electrically and optically. Similar coupling effects of cell parameters in multi-junction solar cells have been reported recently [15]. In a multi-junction solar cell, it is essential to ensure that all subcells remain as closely current matched as possible to maintain high conversion efficiency. The optical coupling in a multi-junction solar cell may lead to the current mismatch between subcells and reduce the conversion efficiency. An understanding of optical coupling is thus important for further optimization of multi-junction solar cells in the design.

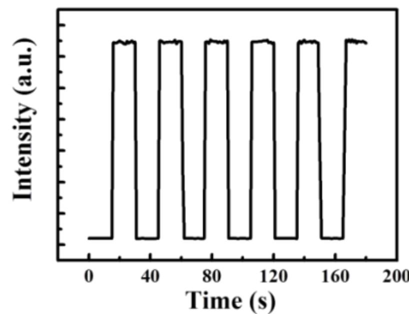

Fig. 9. Time dependence of EL intensity upon the ON-OFF switching of IR light irradiation.

The quenching of EL in the triple-junction solar cells due to IR light is a reversible effect. After stopping IR light irradiation, the dark area disappears immediately and a homogenous EL image recovers. The quenching and reversible effect controlled by IR light imply a photoswitching behavior because quenching of EL was sufficient to switch off EL. Figure 9 shows EL intensity of the InGaP top subcell with the ON-OFF switching of IR light irradiation. As can be seen, one-step ON-OFF EL switching is clearly observed upon IR light

#174226 - $15.00 USD   Received 13 Aug 2012; revised 18 Nov 2012; accepted 25 Nov 2012; published 10 Dec 2012
(C) 2012 OSA

irradiation. The ON-OFF cycles of irradiation confirms the reproducibility of EL response. It is noted that both "ON" and "OFF" states remain stable during excitation of IR light. The optical coupling and photoswitching effects in the multijunction diodes may be used for fabricating an IR image sensor, which have wide application fields. With such devices, large size IR images are easily grabbed without moving parts. This type of IR image sensors is free-of-array and thus simplifies the fabrication process and reduces the production cost. In addition, the multijunction diodes can be monolithically integrated with other III-V optical devices to form a hybridized system. The multijunction diodes demonstrated here are thus of great potential for high quality imaging applications.

In summary, EL in the top subcell of InGaP/InGaAs/Ge solar cells was investigated to demonstrate the coupling from the middle subcell to the top subcell. With increasing the irradiation level of the 1.59-eV IR light, EL intensity quenches exponentially. The coupled p-n junction diode model as well as the photovoltaic effect were used to analyze the quenching mechanism of EL. An understanding of the coupling effects between subcells in InGaP/InGaAs/Ge solar cells may be used for optimizing the conversion efficiency and implementing the infrared sensing applications.

Acknowledgments

This project was supported in part by the Institute of Nuclear Energy Research under grant number 1012001INER024 and by the National Science Council under grant number 100-2811-M-033-014- .

#174226 - $15.00 USD Received 13 Aug 2012; revised 18 Nov 2012; accepted 25 Nov 2012; published 10 Dec 2012
(C) 2012 OSA